Journal of Andrology, Vol. 33, No. 1, January/February 2012
Copyright © American Society of Andrology

Potential Role of Poly(ADP-Ribose) Polymerase Activation in the Pathogenesis of Experimental Left Varicocele

MERIH TEKCAN,* ISMAIL TURKER KOKSAL,† ARDA TASATARGIL,‡ OMER KUTLU,§ ECE GUNGOR,* AND CILER CELIK-OZENCI*

*From the *Department of Histology and Embryology, the †Department of Urology, and the ‡Department of Pharmacology, Akdeniz University, School of Medicine, Antalya, Turkey; and the §Department of Urology, Karadeniz Technical University, School of Medicine, Trabzon, Turkey.*

ABSTRACT: The aim of this study was to evaluate whether the poly(adenosine diphosphate[ADP]–ribose) polymerase (PARP) pathway is activated by experimental left varicocele. Rats underwent partial ligation of the left renal vein to induce experimental varicocele, and left testes were analyzed 13 weeks after surgery. Tubule degeneration was evaluated by Johnsen score. Expression of 4-hydroxy-2-nonenal (4-HNE)–modified proteins, PARP-1, and poly(-ADP-ribose) (PAR) was detected by immunohistochemistry and Western blot. The degree of apoptosis within testes was determined by terminal deoxynucleotidyl transferase–mediated deoxyuridine triphosphate nick end labeling. Light microscopy revealed testicular damage comprising various degrees of seminiferous tubule degeneration. Germ cell apoptotic index and 4-HNE, PAR, and PARP-1 expression in germ cells increased after varicocele induction. Increased oxidative stress and PARP overactivation in testes might be important with regard to impaired testicular function associated with varicocele.

Key words: Oxidative stress, PARP, testes.
J Androl 2012;33:122–132

Varicocele consists of an engorgement and dilatation of the internal spermatic vein and pampiniform plexus above the testes. It has been implicated as a major cause of male infertility in adults (Hauser et al, 2001). Clinical varicocele is observed in 10%–20% of the general male population, whereas it is demonstrated in 19%–41% of men presenting for infertility investigations (Kamal et al, 2001; Naughton et al, 2001). Varicocele is ordinarily accompanied by decreased testicular volume, impaired sperm quality, and a decline in Leydig cell function. However, the exact mechanism by which varicocele produces sperm dysfunction or the pathogenesis of testicular damage has not been clearly defined.

Several theories have been proposed to explain the detrimental effect of varicocele on sperm quality, including the possible effects of oxidative stress. Some studies have demonstrated the increase of superoxide anion and other reactive oxygen species (ROS) in testes of experimental varicocele models (Cam et al, 2004; Ozdamar et al, 2004). These free radicals cause lipid peroxidation and have other deleterious effects on cell structure. Although an association between ROS and varicocele-induced testicular damage was proposed, the downstream cellular mechanisms involved after ROS generation in testes with varicocele have not yet been clearly recognized.

The poly(adenosine diphosphate[ADP]–ribose) polymerase (PARP) pathway has recently been established as a major downstream intracellular pathway of oxidative stress (Radovits et al, 2007). Oxidant species are endogenous inducers of DNA single-strand breakage and are required for PARP activation (Garcia Soriano et al, 2001). Overactivation of PARP represents an important mechanism of tissue damage in various pathological conditions related to oxidative stress (Oliver et al, 1999; Pacher et al, 2002; O'Valle et al, 2005). Activation of PARP results in a rapid depletion of intracellular NAD^+ and adenosine triphosphate (ATP), slows the rate of glycolysis and mitochondrial respiration and eventually leads to cellular dysfunction and death (Pieper et al, 2000; Garcia Soriano et al, 2001).

PARP has been detected in the nuclei of a variety of tissue types, including the brain, heart, kidney, and testis (Poirier et al, 1982; Di Meglio et al, 2004). Di Meglio and others (2003, 2004) have reported higher levels of PARP enzymes in primary spermatocytes undergoing

Supported by Akdeniz University Research Foundation, project 2007.02.0122.014.

Correspondence to: Dr Ciler Celik-Ozenci, Department of Histology and Embryology, Faculty of Medicine, Akdeniz University, 07070 Antalya, Turkey (e-mail: cilerozenci@akdeniz.edu.tr).

Received for publication October 15, 2010; accepted for publication February 15, 2011.
DOI: 10.2164/jandrol.110.012203

Table 1. *Body and testis weights of animals in control, sham, and varicocele groups*[a]

	Left Testis Weight, g	Body Weight, g	Left Testis Weight/Body Weight
Control	2.018 ± 0.03	386.2 ± 7.6	0.0052 ± 0.0001
Sham	1.952 ± 0.03	375.7 ± 13.3	0.0053 ± 0.0002
Varicocele	1.467 ± 0.01[b]	335.8 ± 9.8	0.0044 ± 0.0003[b]

[a] Data are presented as $\bar{x}$ ± SEM; n = 12 for all groups.
[b] $P < .05$.

meiotic division, which has been also supported by the findings of Tramontano et al (2005) (Meyer-Ficca et al, 2005). Detection of poly(ADP-ribose) (PAR) expression in human germ cells demonstrated modification of chromatin during spermatogenesis and establishes a key role for poly(ADP-ribosyl)ation in germ cell differentiation, presumably to safeguard DNA integrity (Maymon et al, 2006). The presence of PARP and its homologues has also been shown in male germ cells, specifically during stage VII of spermatogenesis (Agarwal et al, 2009). Whenever strand breaks occur in sperm DNA from oxidative stress, PARP is activated (El-Domyati et al, 2010). Presence of higher levels of cleaved PARP, a marker of apoptosis, in sperm of infertile men indicates the potential role of PARP as a new marker of sperm damage (Agarwal et al, 2009). Infertile varicocele patients show an increase in human testicular germ cell DNA repair and apoptosis, with a profile resembling premature aging (El-Domyati et al, 2009, 2010). Taking the above into account, activation of the PARP pathway as a consequence of oxidative stress might cause varicocele-induced testicular damage and sperm dysfunction. This study was undertaken to investigate the possible role of PARP pathway activation in the pathogenesis of infertility in a rat model of varicocele.

Materials and Methods

A total of 36 adult Wistar male rats were housed at 24°C under controlled conditions with free access to standard rat chow and water. The experimental protocol was approved by the Animal Care and Usage Committee of Akdeniz University and was in accordance with the Declaration of Helsinki and International Association for the Study of Pain guidelines.

Experimental Varicocele

Twenty-week-old adult animals were used for the control group (n = 12). Animals underwent sham operation at 7 weeks and were studied 13 weeks later (n = 12). Animals in the experimental group underwent partial ligation of the left renal vein at 7 weeks and were studied 13 weeks later. A total of 15 animals were included for the varicocele surgery, and 12 of them developed varicoceles. The establishment of the control and experimental groups are described elsewhere (Turner, 2001). After identification of left varicocele by observation of the dilatation of the internal spermatic veins, both testicles then were harvested from the same incision. Sham-operated rats underwent a similar procedure: the left renal vein was dissected free but was not ligated. Body weights and testes weights from control, sham-operated, and varicocele-induced adult rats were obtained. Animals were killed 13 weeks after renal vein ligation, and left testicular tissues were removed for immunohistochemistry and Western blot analysis. From each animal, left testicular tissues from 6 animals were fixed in Bouin's fixative, dehydrated in ethanol, and embedded in paraffin wax for immunohistochemistry, and 6 left testes from other animals were frozen in liquid nitrogen for Western blot analysis.

Histological Evaluation

Left testicular tissues were stained with hematoxylin and eosin for histopathological evaluations. Tubule degeneration was evaluated in each group by a modified Johnsen score, as described previously (Mizuno et al, 2007).

DAPI Staining

Testicular sections from the varicocele group were stained with 4′,6-diamidino-2-phenylindole (DAPI) nuclear counterstain to see the distribution of DNA in symplasts. A working solution (100 ng/mL DAPI in phosphate-buffered saline [PBS]) prepared from DAPI stock solution (5 mg/mL DAPI in PBS) was used to perform DAPI staining. Sections were incubated in dark for 5 minutes at room temperature.

Immunohistochemistry

Sections were deparaffinized and blocked for endogenous peroxidase activity with methanol containing 3% H_2O_2 for 10 minutes and for nonspecific binding with Ultra V Block (Labvision, Freemont, California) for 7 minutes at room temperature. Mouse monoclonal PAR (anti-PAR Mab (10H), Alexis, San Diego, California) and rabbit polyclonal PARP-1 (Ab 6079, Abcam, Cambridge, Massachusetts) primary antibodies were applied in a dilution of 1.8 μg IgG_3/mL (1:500 dilution) and 6 μg IgG/mL (1:300), respectively, and incubated overnight at +4°C in a humidified chamber. The sections were washed in PBS and incubated with biotinylated horse anti-mouse IgG and anti-rabbit IgG (3 mg/mL; Vector, Burlingame, California) at 1:500 dilution for 45 minutes at room temperature. The antigen-antibody complex was detected by using an avidin-biotin horseradish peroxidase complex with a Universal LSAB Kit (Dako, Glostrup, Denmark). Diaminobenzidine (3,3-diaminobenzidine tetrahydrochloride dihydrate; Sigma, St Louis, Missouri) was used as the

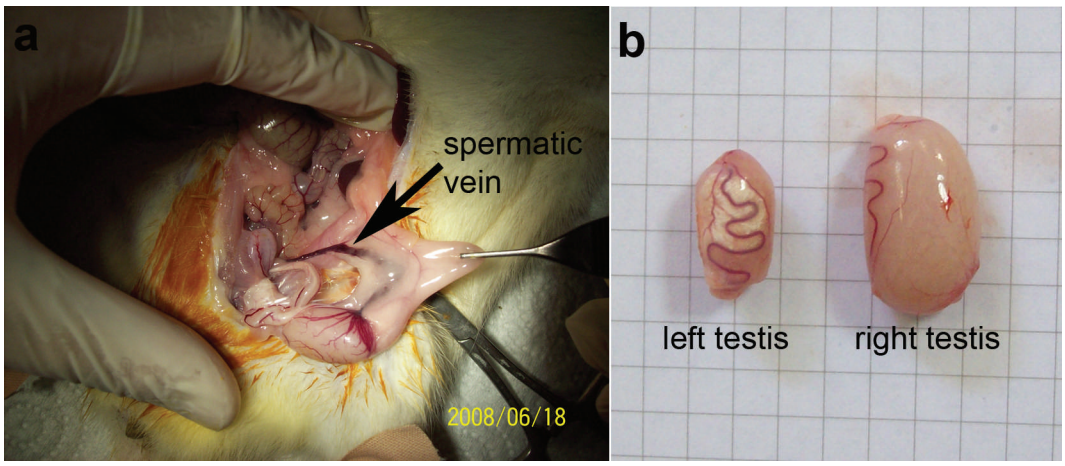


Figure 1. Photographic images of enlarged spermatic vein **(a)** and left and right testes **(b)** of varicocele-induced rats. Compare the sizes of left and right testes of the same animal. Color figure available online at www.andrologyjournal.org.

chromogen, and sections were mounted with Permount (Fisher Chemicals, Zurich, Switzerland) on glass slides and then evaluated under a light microscope. For controls, sections were incubated with non-immune IgG_3 (MAB007, R&D Systems, Minneapolis, Minnesota) and rabbit serum (X0902, Dako) at the same concentrations with primary antibodies. Pictures were taken with an Axiophot microscope (Zeiss, Oberkochen, Germany).

Western Blotting

After homogenization, left testis supernatants were collected and protein concentrations were determined. Each lane received 20 μg protein for 4-hydroxy-2-nonenal (anti-4HNE), 50 μg protein for PAR, and 100 μg protein for PARP-1. Samples were then subjected to sodium dodecyl sulfate polyacrylamide gel electrophoresis under standard conditions and then transferred onto polyvinylidene difluoride membrane. The membranes were blocked for 1 hour with 5% nonfat dry milk and were then incubated overnight at 4°C with the rabbit polyclonal PARP-1 (Ab 6079, Abcam) primary antibody (dilution, 1:300) and mouse monoclonal PAR (anti-PAR Mab (10H), Alexis) primary antibody (dilution, 1:400) for the evaluation of PARP activity and the mouse anti-4HNE Mab (HNEJ-2, JaICA, Fukuroi, Shizuoka, Japan) primary antibody (dilution, 1:100) for the evaluation of oxidative stress. As an internal standard to confirm the equal loading of the proteins, β-actin was loaded to the gels. Intensity measurements of the protein expressions were performed by Alpha Digidoc software (Alpha Innotech Corp, San Leandro, California).

TUNEL

Paraffin sections of 5 μm thickness from testis tissues were washed twice in PBS for 5 minutes. After incubation of slides with the permeabilization solution (0.1% Triton X-100 in 0.1% sodium citrate) for 8 minutes at 4°C and washing twice with PBS for 5 minutes, the labeling reaction was performed with 50 μL of terminal deoxynucleotidyl transferase–mediated deoxyuridine triphosphate nick end labeling (TUNEL) reagent for each sample, except negative control, in which reagent without enzyme was added and incubated for 1 hour at 37°C. After PBS washings, slides were incubated with converter reagent for 30 minutes at 37°C. Color development for localization of cells containing labeled DNA strand breaks was performed by incubating the slides with Fast Red substrate solution for 5 minutes. TUNEL was conducted with the use of a cell death detection kit (Roche, Mannheim, Germany). Apoptotic index was determined by Zeiss Axioplan Microscope. All seminiferous tubules from each group were observed, and the numbers of TUNEL-positive and TUNEL-negative seminiferous tubules were recorded. The seminiferous tubules with apoptotic cell signals were defined as positive seminiferous tubules. The positive seminiferous tubule rate was calculated by multiplying the ratio of positive tubules to total number of tubules by 100.

→

Figure 2. Images of control **(a)**, sham **(b)**, and varicocele-induced **(c–h)** testes stained with hematoxylin and eosin. In control and sham-operated groups, normal tubules are seen **(a, b)**. On the other hand, histopathological evaluations clearly indicate disruption of spermatogenesis in varicocele-induced testes **(c–h)**. Besides normal tubules, disrupted tubules can be seen, indicated by DT **(c)**. A tubule arrested in the round spermatid stage (RSA) and 2 tubules arrested in the primary spermatocyte stage (PSA) consist of immature germ cells **(d)**. Moreover, a Sertoli cell–only tubule (SCO) **(e)** and a tubule consisting of multinuclear giant cells (symplasts) **(f)** are seen in varicocele-induced testes. 4′,6-Diamidino-2-phenylindole nuclear staining of varicocele groups verify the abnormal nuclear materials of symplasts with halo appearance **(g, h)**. Arrows indicate symplasts. Color figure available online at www.andrologyjournal.org.

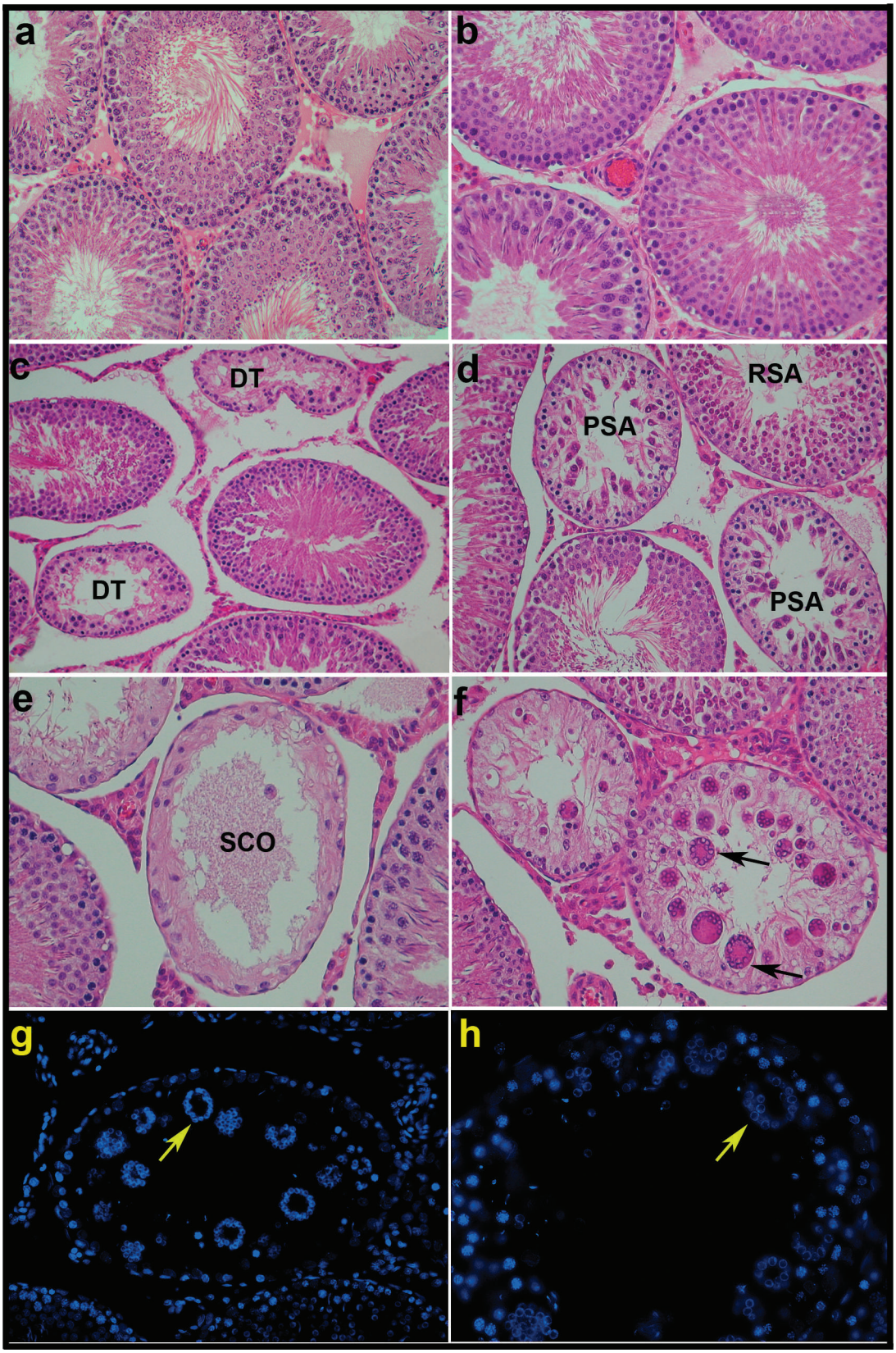

a
b
c
DT
DT
d
RSA
PSA
PSA
e
SCO
f
g
h

Table 2. *Johnsen scores of control, sham, and varicocele groups*[a]

	Control	Sham	Varicocele
Johnsen score	9.4 ± 0.03	9.3 ± 0.04	7.4 ± 0.1[b]
No. of tubules evaluated	400.3 ± 6.8	405.4 ± 5.2	400.2 ± 6.9

[a] Data are presented as $\bar{x}$ ± SEM; n = 6 for all groups.
[b] $P < .05$.

Statistical Analysis

Data are presented as $\bar{x}$ ± SEM and were analyzed by GraphPad Prism™ software version 3.0 (San Diego, California). Significant findings were further compared by 1-way analysis of variance with Tukey posttest. Levels of significance were set at $P < .05$.

Results

Evaluation of the Varicocele Model

The body weights of control, sham, and varicocele-induced rats did not change, whereas left testis weights of the varicocele group decreased significantly (Table 1, Figure 1). The ratio of left testis/body weight in varicocele-induced rats decreased significantly, indicating the testicular tissue loss.

When the testicular sections were evaluated by light microscopy, seminiferous tubules of control and sham-operated rat testes showed normal spermatogenesis with normal testicular histology (Figure 2a and b). However, abnormal spermatogenic cell types in damaged seminiferous tubules were observed in varicocele-induced rats (Figure 2c through h). In addition to seminiferous tubules arrested in the primary spermatocyte stage and in the round spermatid stage (Figure 2d), tubules consisting of only Sertoli cells (Sertoli cell–only tubules) were also present in the varicocele group (Figure 2e). Moreover, symplasts, multinuclear cells within a large cytoplasm, were present in varicocele-induced rat testes (Figure 2f). Additionally, seminiferous tubules containing round spermatids with nuclear condensation failure appeared as a ''halo effect'' (Figure 2f). A DAPI nuclear staining confirmed that genetic material of halo sperm was localized only at the periphery of the cell nuclei (Figure 2g and h).

A significant decrease in mean value of Johnsen scores of varicocele-induced testes confirmed the testicular damage (Table 2).

Immunohistochemistry of PARP-1 and PAR

Immunohistochemical staining of control (Figures 3a and b and 4a and b) and sham (Figures 3c and d and 4c and d) seminiferous tubules with complete spermatogenesis disclosed a pronounced expression of PARP-1 and PAR (end product of PARP activation) in the nuclei of germ cells. Analysis of the subcellular localization of PARP-1 enzyme in tubules with complete spermatogenesis revealed the strongest levels of immunostaining as being localized in spermatogonia and in primary spermatocytes (Figure 3a and b). In comparison, different expression patterns of immunoreactivity for the PAR polymer were found in those tubules. Spermatogonia, which were highly immunoreactive for PARP-1, also exhibited strong PAR expression (Figure 4a and b), in addition to the slight PAR expression in elongating spermatids at stages X through XII (Figure 4a and b). Expressions of PARP-1 and PAR proteins in control and sham groups with regard to seminiferous tubule stage and cell type are summarized in Figure 5a.

In the varicocele group, expressions of both PARP-1 and PAR proteins increased considerably (Figures 3e and f and 4e and f). At stages I through VII, both PARP and PAR expressions were present in spermatogonia, primary spermatocytes, and round spermatids. Expressions of PARP-1 and PAR proteins in the varicocele group with regard to seminiferous tubule stage and cell type are summarized in Figure 5b.

Western Blot Findings

Western blot findings confirmed the results of immunohistochemistry. An oxidative stress marker, 4-HNE, significantly increased in the varicocele group (Figure 6). Additionally, expressions of both PARP-1 and PAR proteins increased markedly in varicocele-induced rats compared with sham and control groups (Figure 6a and b). In control and sham groups, the full-length form of PARP-1 (corresponding to 113 kd molecular weight) was present. On the other hand, in varicocele-induced testes, PARP-1 expression revealed 2 bands corresponding to 113 kd (full-length form) and 29 kd (cleaved form) molecular weights. The expression of full-length PARP-1 increased significantly in the varicocele-induced group when compared with the control and sham groups. Moreover, the presence of the apoptotic form of PARP-1 (29 kd) in varicocele testes indicated cleavage of the overexpressed PARP-1 protein.

TUNEL

When compared with the control and sham groups, the number of apoptotic cells increased significantly in varicocele-induced testes (Figure 7a and b).

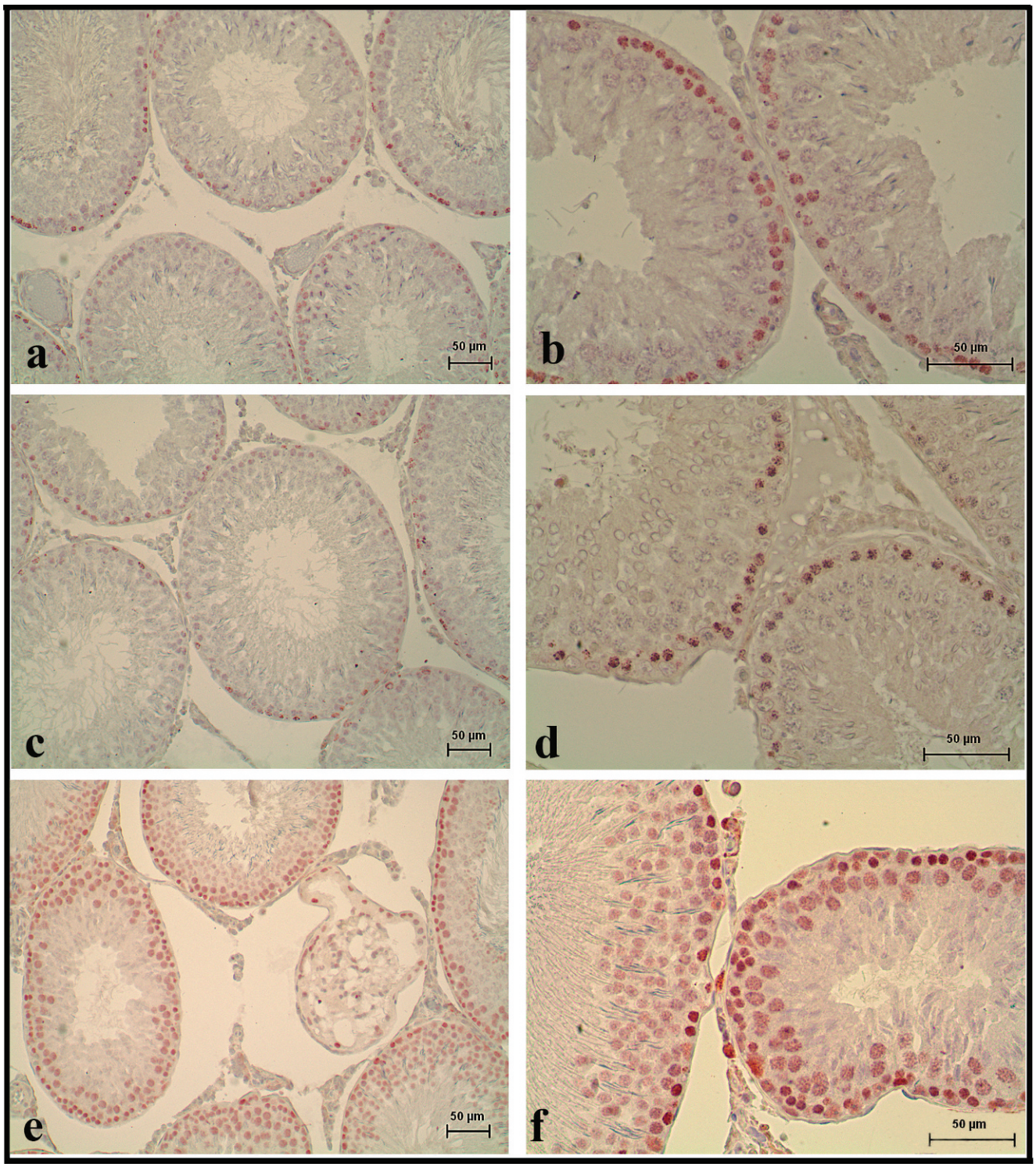


Figure 3. Representative photomicrographs for poly(adenosine diphosphate–ribose) polymerase (PARP)–1 immunohistochemistry in control **(a, b)**, sham **(c, d)**, and varicocele-induced **(e, f)** testes. Strong immunostaining of PARP-1 **(e, f)** was observed in germ cells of varicocele-induced groups. In sham-operated rats, the expression of PARP-1 **(c, d)** in germ cells was similar to controls **(a, b)**. Color figure available online at www.andrologyjournal.org.

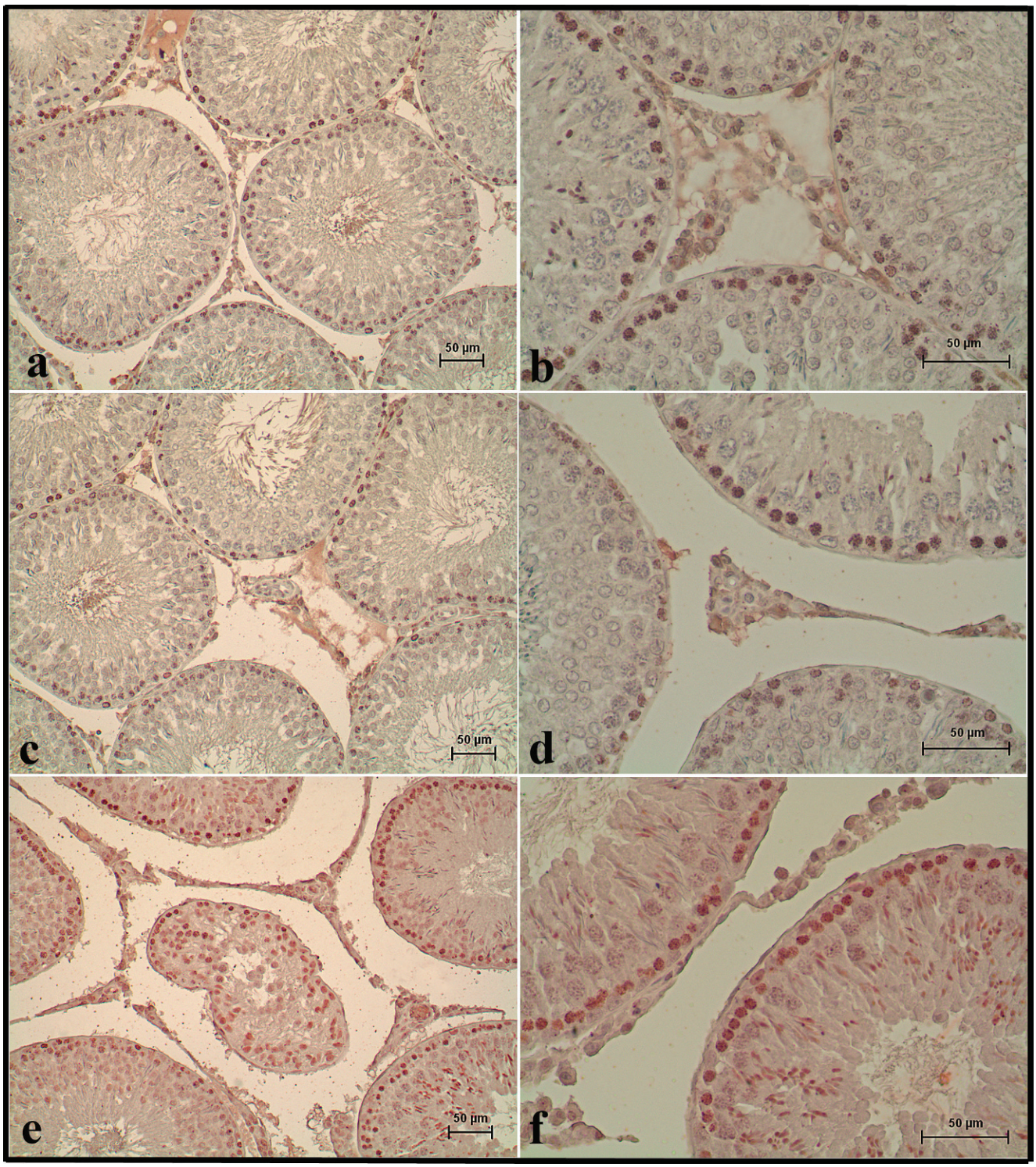


Figure 4. Representative photomicrographs for poly(adenosine diphosphate[ADP]-ribose) (PAR) immunohistochemistry in control **(a, b)**, sham **(c, d)**, and varicocele-induced **(e, f)** testes. Strong immunostaining of PAR **(e, f)** was observed in germ cells of varicocele-induced groups. In sham-operated rats, the expression of poly(ADP–ribose) polymerase–1 **(c, d)** in germ cells was similar to controls **(a, b)**. Color figure available online at www.andrologyjournal.org.

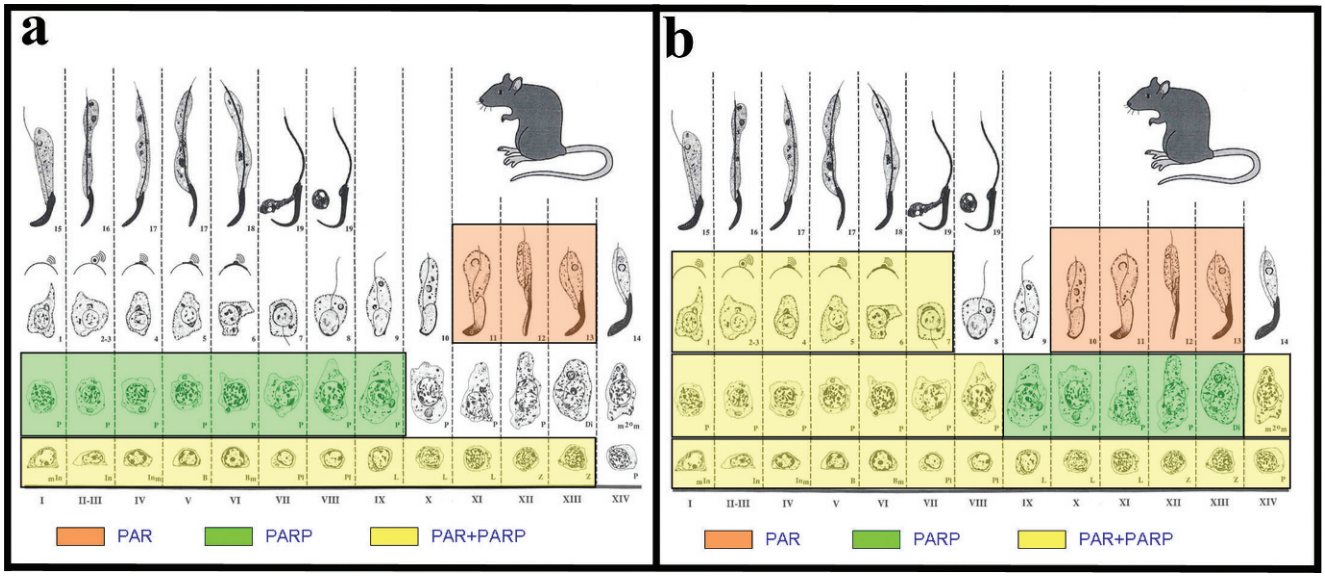


Figure 5. Summary of poly(adenosine diphosphate[ADP]–ribose) polymerase (PARP)–1 and poly(ADP-ribose) (PAR) localizations in control and sham **(a)** and in varicocele-induced **(b)** rat testes. Adult rat testis staging diagram depicting PARP-1 (green) and PAR (orange) localization. Yellow color indicates co-localization of PARP-1 and PAR in germ cells of the seminiferous tubules. Details of symbols used in the staging maps shown can be found in Russell et al (1987). This material is reprinted with permission of John Wiley & Sons Inc. Color figure available online at www.andrologyjournal.org.

Discussion

The present study was carried out to investigate the role of the PARP pathway in the pathogenesis of varicocele-induced testicular damage. It is important to remember that surgically induced varicocele in animals in vivo does not completely mimic varicocele in humans, but it is widely used to evaluate possible mechanisms underlying this condition. To date, several factors have been proposed to account for varicocele-induced testicular injury. Our study is the first that examines the role of the PARP pathway in varicocele-induced damage in rat testes.

Our histological findings indicated an extensive degeneration of seminiferous tubules in varicocele groups. Histopathological evaluations clearly showed degeneration of spermatogenesis in varicocele-induced testes, including tubules arrested at the round spermatid and spermatocyte stages. Recently, susceptibility during the spermatocyte stages has also been seen in varicocele testes of humans (El-Domyati et al, 2009, 2010). In addition to Sertoli cell–only tubules, tubules consisting of multinucleated giant cells or symplasts, as described by Russell et al (1987), were present in varicocele groups. The mechanism of varicocele-induced testicular damage has not yet been fully established; however, it is thought that oxidative damage plays an important role in this condition (Koksal et al, 2000; Agarwal et al, 2009). Although the association between oxidative stress and testicular damage in varicocele is partly investigated, the downstream cellular mechanisms involved after elevation of oxidative stress are still unknown. However, elevation of ROS, induction of DNA injury, and subsequent activation of PARP pathway has recently been established as a major downstream intracellular pathway of nitrosative and oxidative stress (Radovits et al, 2007). It is well known that the catalytic activity of the nuclear enzyme PARP, induced by breakage of single-strand DNA, is a direct result of oxidant injury (Schraufstatter et al, 1986). Oxidative stress accompanied by increased formation of superoxide anions, hydrogen peroxide, and peroxynitrite induces single-strand DNA breakage and PARP activation, leading to cellular dysfunction and necrosis by rapid depletion of intracellular NAD^+ and ATP pools (Pieper et al, 2000; Hassa and Hottiger, 2002). PARP is involved in the repair process of DNA but uses NAD^+, as a substrate. Subsequently, cells utilize ATP to regenerate NAD^+ stores.

Our study showed that oxidative stress increased in varicocele-induced left testes. It is well known that PARP activity increases with oxidative stress. Our immunohistochemical findings indicated that both PARP-1 and PAR expression in germ cells increased as well. The expression patterns of the enzyme PARP-1 and PAR were somewhat similar to each other. In control and sham groups, PARP-1 was present in

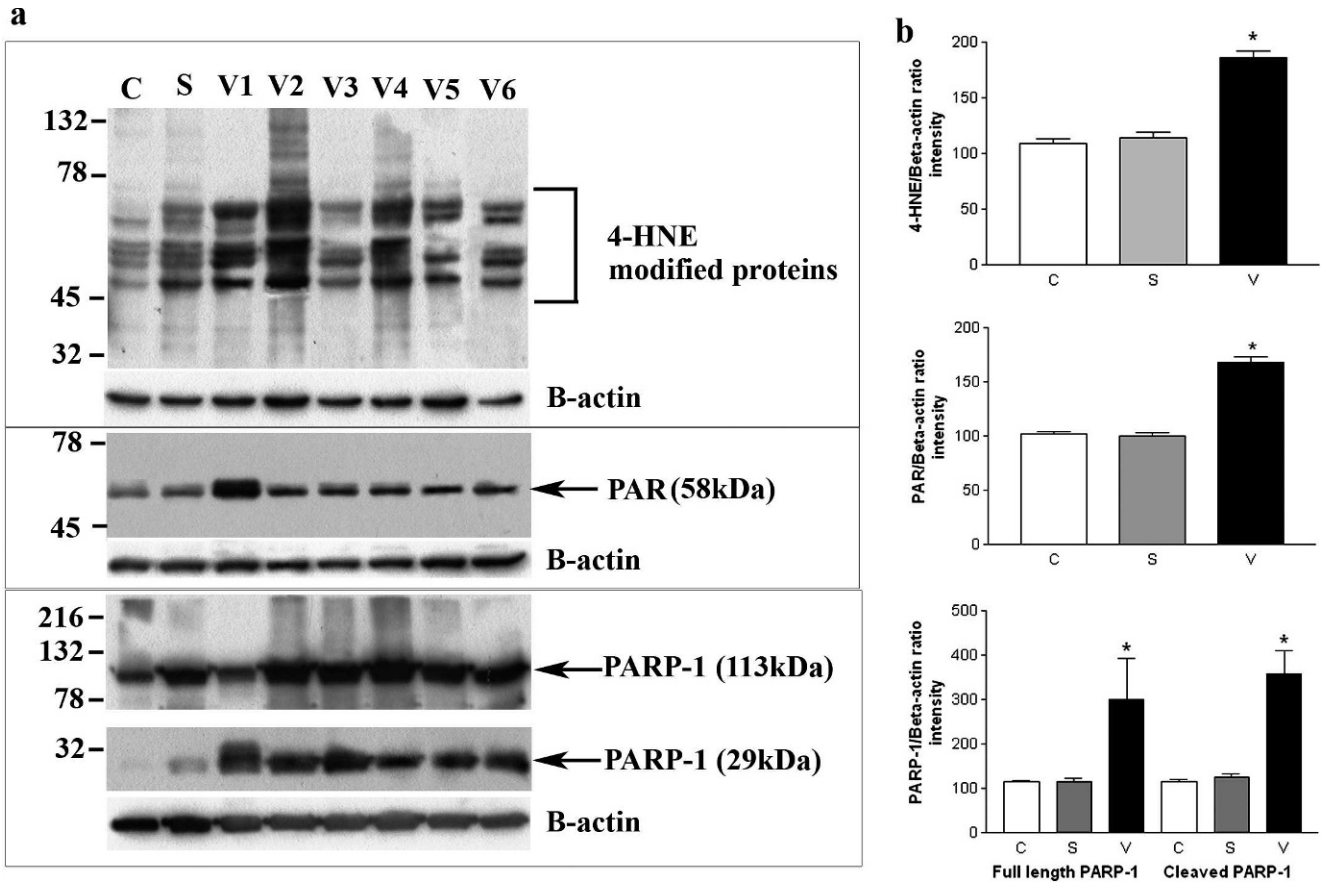


Figure 6. Evaluation of 4-hydroxy-2-nonenal (4-HNE), poly(adenosine diphosphate[ADP]–ribose) polymerase (PARP)–1, and poly(ADP-ribose) (PAR) expressions of left testes tissues by Western blot analysis in control, sham, and varicocele-induced rats **(a)**. Oxidative stress marker 4-HNE, PARP-1, and PAR activity increased in varicocele groups. Quantitative analysis of protein expressions are presented as graphics **(b)**. β-Actin was loaded to the gels as an internal standard to confirm the equal loading of the proteins. C indicates control; S, sham-operated; V1–V6, varicocele-induced. * $P < .05$.

spermatogonia and spermatocytes, indicating its possible role in stem cells of the testis and meiotic processes. In contrast, PAR was localized to spermatogonia and elongating spermatids only, indicating the contribution of poly(ADP)ribosylation during stem cell activity and chromatin modeling of elongating rat sperm. In the varicocele group, expressions of PARP-1 and PAR increased, and cellular localizations of these proteins changed. PARP-1 was expressed in spermatogonia, spermatocytes, and round spermatids. Similarly, PAR was immunolocalized to spermatogonia, spermatocytes, round spermatocytes, and elongating spermatocytes, which could indicate that the shutdown of protein expression for PARP-1 and PAR was delayed in varicocele, leading to overactivation of PARP-1 and PAR. In accordance with these results, the quantitative analysis of PARP-1 and PAR by Western blot indicated an increase in the varicocele group when compared with control and sham groups.

It is well known that PARP-1 is cleaved in fragments of 89 and 24 kd during apoptosis (Gobeil et al, 2001). During apoptosis, cleavage of PARP-1 in fragments of 89 and 24 kd has become a useful hallmark of this type of cell death (Kaufmann et al, 1993). Cleavage of PARP might prevent its overactivation, energy depletion, and necrosis by preserving cellular energy required for the apoptotic mode of cell death. Our results clearly indicate that the cleavage of a 113-kd PARP to a 29-kd fragment occurs in germ cells in varicocele-induced rats. It is most likely that increased oxidative stress in varicocele-induced testicular tissue might be responsible for the cleavage of full-length PARP into its apoptotic fragment. Accordingly, the number of apoptotic cells increased in germ cells of varicocele-induced rats.

In conclusion, the current study demonstrates directly that PARP-1 is overactivated in germ cells of varicocele-induced rat testes; thus, it might contribute to testicular damage in varicocele.

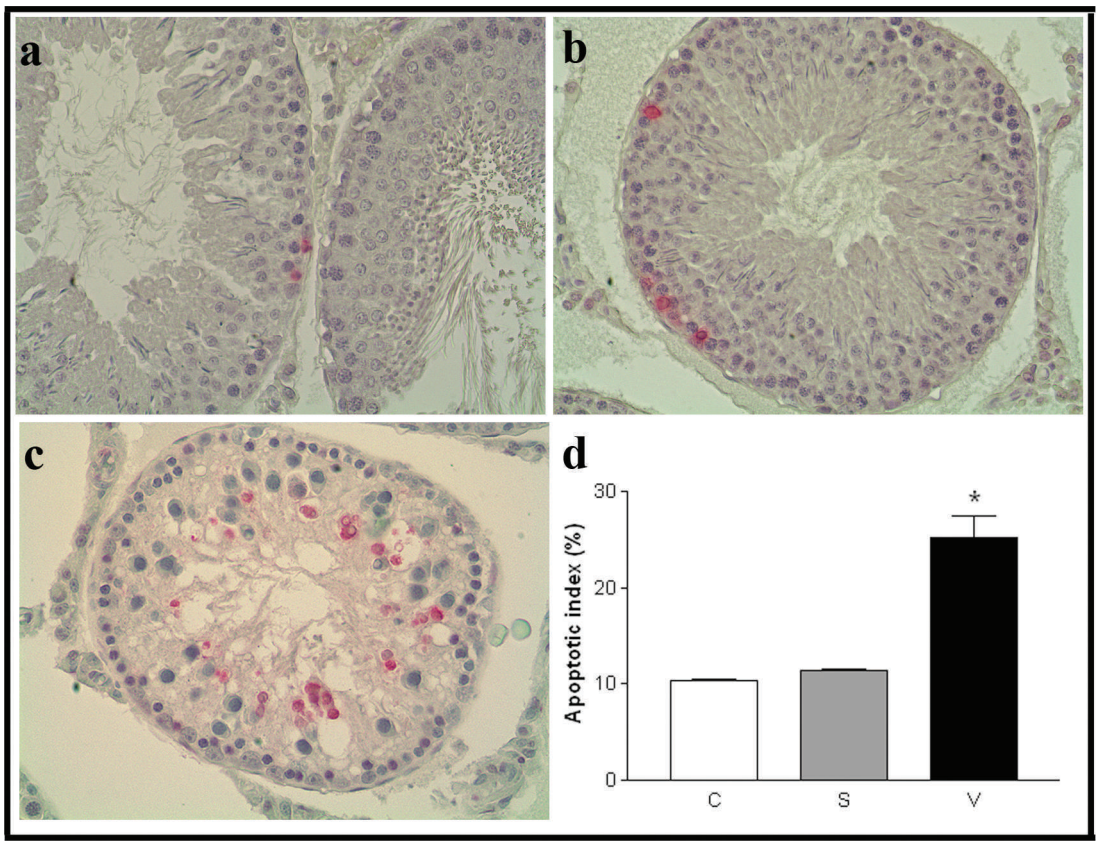


Figure 7. Representative photomicrographs for terminal deoxynucleotidyl transferase–mediated deoxyuridine triphosphate nick end labeling in control (C) **(a)**, sham-operated (S) **(b)**, and varicocele-induced (V) **(c)** testes. Cell death increased in germ cells in varicocele groups determined by apoptotic index **(d)**. * $P < .05$. Color figure available online at www.andrologyjournal.org.

References

Agarwal A, Mahfouz RZ, Sharma RK, Sarkar O, Mangrola D, Mathur PP. Potential biological role of poly (ADP-ribose) polymerase (PARP) in male gametes. *Reprod Biol Endocrinol*. 2009;7:143.

Cam K, Simsek F, Yuksel M, Turkeri L, Haklar G, Yalcin S, Akdas A. The role of reactive oxygen species and apoptosis in the pathogenesis of varicocele in a rat model and efficiency of vitamin E treatment. *Int J Androl*. 2004;27:228–233.

Di Meglio S, Denegri M, Vallefuoco S, Tramontano F, Scovassi AI, Quesada P. Poly(ADPR) polymerase-1 and poly(ADPR) glycohydrolase level and distribution in differentiating rat germinal cells. *Mol Cell Biochem*. 2003;248:85–91.

Di Meglio S, Tramontano F, Cimmino G, Jones R, Quesada P. Dual role for poly(ADP-ribose)polymerase-1 and -2 and poly(ADP-ribose)glycohydrolase as DNA-repair and pro-apoptotic factors in rat germinal cells exposed to nitric oxide donors. *Biochim Biophys Acta*. 2004;1692:35–44.

El-Domyati MM, Al-Din AB, Barakat MT, El-Fakahany HM, Honig S, Xu J, Sakkas D. The expression and distribution of deoxyribonucleic acid repair and apoptosis markers in testicular germ cells of infertile varicocele patients resembles that of old fertile men. *Fertil Steril*. 2010;93:795–801.

El-Domyati MM, Al-Din AB, Barakat MT, El-Fakahany HM, Xu J, Sakkas D. Deoxyribonucleic acid repair and apoptosis in testicular germ cells of aging fertile men: the role of the poly(adenosine diphosphate-ribosyl)ation pathway. *Fertil Steril*. 2009;91:2221–2229.

Garcia Soriano F, Virag L, Jagtap P, Szabo E, Mabley JG, Liaudet L, Marton A, Hoyt DG, Murthy KG, Salzman AL, Southan GJ, Szabo C. Diabetic endothelial dysfunction: the role of poly(ADP-ribose) polymerase activation. *Nat Med*. 2001;7:108–113.

Gobeil S, Boucher CC, Nadeau D, Poirier GG. Characterization of the necrotic cleavage of poly(ADP-ribose) polymerase (PARP-1): implication of lysosomal proteases. *Cell Death Differ*. 2001;8:588–594.

Hassa PO, Hottiger MO. The functional role of poly(ADP-ribose)polymerase 1 as novel coactivator of NF-kappaB in inflammatory disorders. *Cell Mol Life Sci*. 2002;59:1534–1553.

Hauser R, Paz G, Botchan A, Yogev L, Yavetz H. Varicocele: effect on sperm functions. *Hum Reprod Update*. 2001;7:482–485.

Kamal KM, Jarvi K, Zini A. Microsurgical varicocelectomy in the era of assisted reproductive technology: influence of initial semen quality on pregnancy rates. *Fertil Steril*. 2001;75:1013–1016.

Kaufmann SH, Desnoyers S, Ottaviano Y, Davidson NE, Poirier GG. Specific proteolytic cleavage of poly(ADP-ribose) polymerase: an early marker of chemotherapy-induced apoptosis. *Cancer Res*. 1993;53:3976–3985.

Koksal IT, Tefekli A, Usta M, Erol H, Abbasoglu S, Kadioglu A. The role of reactive oxygen species in testicular dysfunction associated with varicocele. *BJU Int*. 2000;86:549–552.

Maymon BB, Cohen-Armon M, Yavetz H, Yogev L, Lifschitz-Mercer B, Kleiman SE, Botchan A, Hauser R, Paz G. Role of poly(ADP-ribosyl)ation during human spermatogenesis. *Fertil Steril*. 2006;86:1402–1407.

Meyer-Ficca ML, Scherthan H, Burkle A, Meyer RG. Poly(ADP-ribosyl)ation during chromatin remodeling steps in rat spermiogenesis. *Chromosoma*. 2005;114:67–74.

Naughton CK, Nangia AK, Agarwal A. Pathophysiology of varicoceles in male infertility. *Hum Reprod Update*. 2001;7:473–481.

Mizuno K, Hayashi Y, Kojima Y, Kurokawa S, Sasaki S, Kohri K. Influence for testicular development and histological peculiarity in the testes of flutamide-induced cryptorchid rat model. *Int J Urol*. 2007;14:67–72.

Oliver FJ, Menissier-de Murcia J, Nacci C, Decker P, Andriantsitohaina R, Muller S, de la Rubia G, Stoclet JC, de Murcia G. Resistance to endotoxic shock as a consequence of defective NF-kappaB activation in poly (ADP-ribose) polymerase-1 deficient mice. *EMBO J*. 1999;18:4446–4454.

O'Valle F, Benitez MC, Gomez-Morales M, Bravo J, Osuna A, Del Moral RM, Martin-Oliva D, Oliver FJ, Del Moral RG. Role of poly-(ADP-ribose) polymerase in transplant acute tubular necrosis and its relationship with delayed renal function. *Transplant Proc*. 2005;37:1421–1423.

Ozdamar AS, Soylu AG, Culha M, Ozden M, Gokalp A. Testicular oxidative stress. Effects of experimental varicocele in adolescent rats. *Urol Int*. 2004;73:343–347.

Pacher P, Liaudet L, Bai P, Virag L, Mabley JG, Hasko G, Szabo C. Activation of poly(ADP-ribose) polymerase contributes to development of doxorubicin-induced heart failure. *J Pharmacol Exp Ther*. 2002;300:862–867.

Pieper AA, Walles T, Wei G, Clements EE, Verma A, Snyder SH, Zweier JL. Myocardial postischemic injury is reduced by poly-ADPripose polymerase-1 gene disruption. *Mol Med*. 2000; 6:271–282.

Poirier GG, de Murcia G, Jongstra-Bilen J, Niedergang C, Mandel P. Poly(ADP-ribosyl)ation of polynucleosomes causes relaxation of chromatin structure. *Proc Natl Acad Sci U S A*. 1982; 79:3423–3427.

Radovits T, Zotkina J, Lin LN, Bomicke T, Arif R, Gero D, Horvath EM, Karck M, Szabo C, Szabo G. Poly(ADP-Ribose) polymerase inhibition improves endothelial dysfunction induced by hypochlorite. *Exp Biol Med (Maywood)*. 2007;232:1204–1212.

Russell LD, Vogl AW, Weber JE. Actin localization in male germ cell intercellular bridges in the rat and ground squirrel and disruption of bridges by cytochalasin D. *Am J Anat*. 1987;180:25–40.

Schraufstatter IU, Hinshaw DB, Hyslop PA, Spragg RG, Cochrane CG. Oxidant injury of cells. DNA strand-breaks activate poly-adenosine diphosphate-ribose polymerase and lead to depletion of nicotinamide adenine dinucleotide. *J Clin Invest*. 1986;77:1312–1320.

Tramontano F, Di Meglio S, Quesada P. Co-localization of poly(ADPR)polymerase 1 (PARP-1) poly(ADPR)polymerase 2 (PARP-2) and related proteins in rat testis nuclear matrix defined by chemical cross-linking. *J Cell Biochem*. 2005;94:58–66.

Turner TT. The study of varicocele through the use of animal models. *Hum Reprod Update*. 2001;7:78–84.